

Systematic Search for Electromagnetic Counterparts to the Binary Neutron Star Merger Candidate GW231109_235456

ZHIRUI LI,^{1,2} ZHIWEI CHEN,^{1,2} YANG HUANG,^{2,1} YOUJUN LU,^{1,2} AND JIFENG LIU^{1,2}

¹*National Astronomical Observatories, Chinese Academy of Sciences, Beijing 100012, P.R. People's Republic of China.*

²*School of Astronomy and Space Science, University of Chinese Academy of Sciences, Beijing 100049, People's Republic of China.*

ABSTRACT

In this letter, we present a systematic search for the electromagnetic counterparts of binary neutron star (BNS) merger candidate GW231109.235456 by examining all transients reported within the 90% probability region and detected within four days of the merger. While non-detection in γ -ray, we identify two optical candidates, each associated with and residing in a host galaxy, which locate within 330 Mpc from earth; notably, one of them, AT2023xqy, is located at a distance of 178.6 Mpc, in good agreement with the estimated distance of the GW candidate ($\sim 165^{+70}_{-69}$ Mpc). Near the trigger time of GW231109.235456 (MJD 60257.996), AT2023xqy showed evidence of a ~ 15 -day rise, first detected at 3σ significance on MJD 60259.097 and confirmed above 5σ on MJD 60262.088. This was followed by a rapid ~ 5 -day decline and a plateau lasting at least 50 days, with the subsequent decay unobserved due to a data gap. The spatiotemporal coincidences indicate that AT2023xqy could be a candidate for the EM counterpart of BNS merger candidate GW231109.235456, though its lightcurve is difficult to reconcile with a standard kilonova. We examine two possible scenarios to explain the origin of AT2023xqy, a BNS merger-irrelevant scenario involving a peculiar supernova or a BNS merger-relevant scenario involving a magnetar-powered kilonova under extreme conditions. Follow-up radio observations are strongly encouraged, as they may provide critical insights into the nature of AT2023xqy.

Keywords: Gravitational wave astronomy (675) — Gravitational wave sources (677)

1. INTRODUCTION

Binary neutron star (BNS) mergers are prime targets in multi-messenger astrophysics, as they generate both gravitational wave (GW) signals and electromagnetic (EM) counterparts such as kilonovae, short Gamma Ray bursts (sGRBs) and multi-band afterglows. The landmark event GW170817, detected by LIGO (Aasi et al. 2015) and Virgo (Acernese et al. 2015) over eight years ago, was accompanied by both the sGRB GRB170817A and kilonova AT2017gfo, with extensive follow-up observations across the entire EM spectrum (Abbott et al. 2017a,b,c). These multi-messenger observations provided unprecedented insights into r-process nucleosyn-

thesis (Kasen et al. 2017), the formation and structure of relativistic jets (Mooley et al. 2018), and the dynamics of compact object mergers (Gill et al. 2019). In contrast, the second reported BNS merger candidate, GW190425 (Abbott et al. 2020), lacked a confirmed EM counterpart, highlighting the difficulty of capturing such signals from these events.

The ongoing fourth observing run of the LIGO–Virgo–KAGRA (LVK) network, which began in May 2023, offers unprecedented sensitivity to GW events (Soni et al. 2025; Capote et al. 2025; Ganapathy et al. 2023). However, no confident BNS candidates have been reported in real-time searches or in the latest Gravitational Wave Transient Catalog (GWTC-4.0; Abac et al. 2025). The LVK official pipelines are designed to detect not only BNS, but also binary black hole (BBH) and neutron star–black hole (NSBH) mergers. In such cases, weak BNS signals that would otherwise be consistent with realistic BNS populations can fall below detection thresholds due to the non-optimized population priors. These sub-threshold mergers may

Corresponding author: Zhiwei Chen, Yang Huang and Youjun Lu
chenzhiwei171@mails.ucas.ac.cn

huangyang@ucas.ac.cn

luyj@nao.cas.cn

Table 1. 8 transients within 90% probability area < 4 days post-GW detection.

Designation	R.A. (J2000.0) Dec. (J2000.0)	Date of Discovery MJD	Mag. at Discovery Filter	Host Galaxy Redshift z
AT2023abkc	23:53:50.789 −28:09:41.22	2023-11-10 05:32:09.024 60258.23066	20.40 PanSTARRS w_{P1}	PGC 744988 0.1075
AT2023xqf	00:03:55.159 −29:35:38.95	2023-11-10 10:40:28.128 60258.44477	20.08 GOTO L	—
AT2023xpx	23:38:49.625 −29:40:58.84	2023-11-11 10:09:02.016 60259.42294	19.17 GOTO L	PGC 726409 (AGN) 0.1026
AT2023xnj	00:21:31.492 −32:48:20.18	2023-11-11 10:45:19.296 60259.44814	20.25 GOTO L	PGC 685271 0.176±0.021 (photo- z)
AT2023acmp	00:14:18.685 −30:23:38.80	2023-11-12 03:09:29.000 60260.13159	26.02 JWST other	A2744cl 1447 1.1613
AT2023xsx	00:45:48.771 −28:48:25.65	2023-11-12 22:48:42.336 60260.95049	19.114 ATLAS c	PGC 737216 0.070±0.013 (photo- z)
AT2023xqy	23:41:43.058 −34:12:06.46	2023-11-13 11:06:02.592 60261.46252	19.32 GOTO L	ESO 408-16 / PGC 72135 0.0390
AT2023xsy	23:35:35.668 −40:12:40.81	2023-11-13 19:55:11.136 60261.82999	19.49 ATLAS c	PGC 2794577 0.1273

still produce observable EM counterparts, motivating the need for refined search strategies.

Recently, [Niu et al. \(2025\)](#) proposed a search method optimized for sub-threshold GW events using the Galactic double neutron star (DNS) catalog, built from radio observations ([Özel & Freire 2016](#)), as a representative BNS population. Because this population is considerably narrower than the broad parameter space explored in O4a ([Abac et al. 2025](#)), this approach can enhance the recovery of BNS signals that might be missed by standard pipelines. Applying this refined search to the first part of LVK’s fourth observing run, [Niu et al. \(2025\)](#) identified a significant trigger with a false-alarm rate of one per 50 years and a network signal-to-noise ratio of 9.7. This event was initially reported in LVK low-latency processing as S231109ci and later included in GWTC-4.0 as GW231109_235456, a sub-threshold BNS candidate. If of astrophysical origin, the inferred source properties suggest component masses of 1.40–2.24 M_{\odot} for the primary and 0.97–1.49 M_{\odot} for the secondary, yielding a total mass of $2.95^{+0.38}_{-0.07} M_{\odot}$. The event was localized to a 450 deg² region (90% probability) at a luminosity distance of 165^{+70}_{-69} Mpc.

In this letter, we present a systematic search for the EM counterparts of GW231109_235456 using archival data. We identify two potential optical transients, with one, namely AT2023xqy lying well within both the sky localization map and the expected luminosity distance. Furthermore, its rising time is consistent with the GW trigger time, making it a plausible EM counterpart candidate to GW231109_235456. The structure of this let-

ter is as organized as follows. In Section 2, we describe the complete procedure for searching the EM counterpart; Section 3 presents the light curves of the potential candidates and interprets them using a simple toy model. Finally, Section 4 summarizes our findings. Throughout this paper, we adopt the cosmological parameters from the Planck 2018 results ([Planck Collaboration et al. 2020](#)).

2. SEARCHING FOR ELECTROMAGNETIC COUNTERPARTS TO GW231109_235456

We performed an initial search for EM counterparts using the Transient Name Server¹. The search region was defined by the all-sky spatial probability density map of GW231109_235456 provided by GraceDB², selecting the area that encloses 90% of the probability. Since both numerical simulations and observations of the only confirmed GWEM counterpart, AT2017gfo, show that emissions from binary neutron star mergers rise steeply and peak within a few days ([Abbott et al. 2017a](#); [Cowperthwaite et al. 2017](#)), we further restricted our candidates to transients reported within four days of GW231109_235456. Specifically, we considered reports between MJD 60257.996 (the detection time of GW231109_235456) and MJD 60261.996.

In parallel, we examined high-energy counterparts using the Fermi-GBM catalog³. No burst was found

¹ <https://www.wis-tns.org/>

² <https://gracedb.ligo.org/>

³ <https://heasarc.gsfc.nasa.gov/W3Browse/fermi/fermigbrst.html>

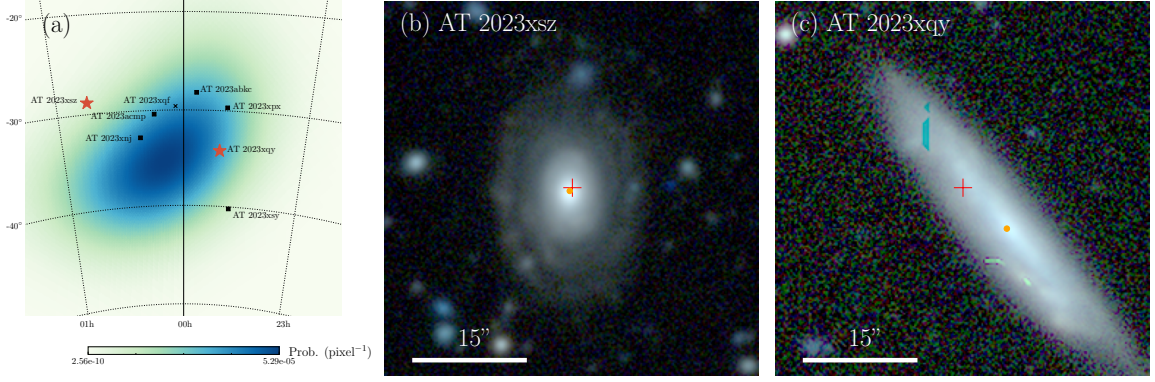


Figure 1. (a) Sky locations of 8 optical candidates. The background color represents the spatial probability distribution of the gravitational-wave event derived from the GW signal, with blue shades indicating higher probability. The cross mark for AT2023xqf indicates that no host galaxy was found in the cross-match. AT2023xsx and AT2023xqy are marked with red stars, denoting that the redshifts of their host galaxies are consistent with the values reported by Niu et al. (2025). Other candidates are marked with black squares. (b) Location of the optical transient AT2023xsx within its host galaxy, PGC 737216. The transient and the host galaxy are marked with a red cross and an orange point, respectively. The background image uses DES DR10 imaging data (Dark Energy Survey Collaboration et al. 2016). (c) Similar to (b) but for AT2023xqy within its host galaxy, PGC 72135. Additionally, two defects are visible in the DES image, with cyan speckles in the upper-left and light-green streaks in the lower-right corner; however, they do not affect our presentation of AT2023xqy and its host galaxy.

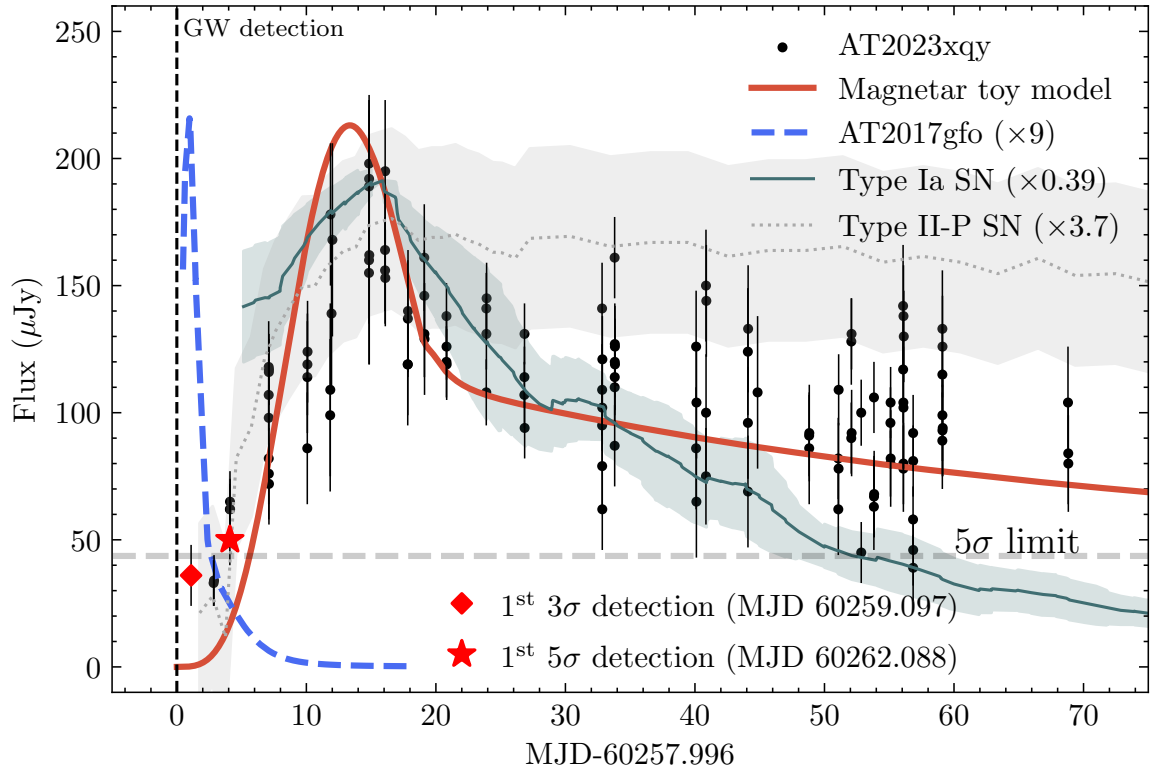


Figure 2. The ATLAS o -band light curve of AT2023xqy with a magnetar toy-model match (solid red line) is compared with a Johnson R -band Type Ia template (cyan solid line with confidence interval), a ZTF r -band Type IIP template (grey dashed line with confidence interval), and the theoretical r -band kilonova light curve of AT2017gfo (blue dashed line). All photometric measurements of AT2023xqy exceed the 3σ detection threshold, with the first 3σ and 5σ detections indicated in the plot. For reference, the 5σ limiting depth under dark-time conditions is $43.65 \mu\text{Jy}$ ($m \approx 19.8$), which is also indicated. The AT2023xqy curve shows the measured fluxes of the source, while the comparison templates have been peak-normalized to highlight differences in light-curve morphology. The Type Ia template is from Jha et al. (2006), the Type IIP curve from Figure 7 of Das et al. (2025), and the kilonova model from Cowperthwaite et al. (2017).

during this interval, except for GRB 231109A (trigger 231109274), which occurred about 17 hours prior to GW231109_235456. Given the temporal offset, it is unlikely to be associated.

By combining the 90% probability sky region and excluding one confirmed Type Ia supernova, we identified a total of eight optical candidates. Of these, four were discovered by the Gravitational-wave Optical Transient Observer (GOTO, [Dyer et al. 2024](#)), two by Asteroid Terrestrial-impact Last Alert System (ATLAS, [Tonry et al. 2018](#)), and one by Pan-STARRS ([Kaiser et al. 2002](#)). An additional candidate, AT2023acmp, was reported by JWST/NIRCam, though the discovery filter was not specified. Except for AT2023acmp, the discovery magnitudes of the remaining seven candidates were all in the range of 19–20 mag. The details of these candidates are listed in Table 1, and their spatial distributions are shown in Figure 1(a).

After cross-matching with the HyperLEDA galaxy catalog ([Paturel et al. 2003](#)) within a 5-arcminute radius, seven optical candidates, including AT2023acmp, which was already identified with its host galaxy, were found to be associated with known galaxies. All of these hosts have either DES DR9 photometric redshift estimates or spectroscopic redshift measurements, as summarized in Table 1. [Niu et al. \(2025\)](#) suggested that the BNS merger lies at a distance of 165^{+70}_{-69} Mpc, corresponding to a redshift of 0.04 ± 0.02 . Based on this, we focused on candidates with host galaxy redshifts below 0.1. This criterion excluded five candidates with higher redshifts, leaving two transients: AT2023xsx with a host DES DR9 photometric redshift of 0.070 ([Sánchez et al. 2014](#); [Dark Energy Survey Collaboration et al. 2016](#)), and AT2023xqy with a host 2dF spectroscopic redshift of 0.0390 ([Colless et al. 2001](#)).

2.1. AT2023xsx

AT2023xsx was first reported by the ATLAS on 2023 November 12. Cross-matching with HyperLEDA places it 0.52 arcseconds (corresponding to 0.7 kpc at its host galaxy redshift) from the center of its host galaxy, PGC 737216 [Figure 1(b)]. In DES images, PGC 737216 appears as a disk galaxy with a ring or spiral arms. DES DR9 provides a photometric redshift of $z = 0.070 \pm 0.013$, corresponding to a luminosity distance of ~ 330 Mpc, slightly beyond the 2σ distance estimate for GW231109_235456 reported by [Niu et al. \(2025\)](#).

The discovery magnitude reported to TNS was 19.114 mag in the ATLAS cyan (*c*) band. The ATLAS light curve ([Smith et al. 2020](#)) shows a peak magnitude of 19.35 ± 0.30 mag in the orange (*o*) band (see Figure A1), while the cyan band is sparsely sampled. The

o-band light curve indicates that AT2023xsx had already brightened by MJD 60259.135 and reached peak brightness near MJD 60262, suggesting a rise time slightly longer than 3 days. However, as its brightness was close to the ATLAS 5σ detection limit (~ 19 mag), the data quality is relatively poor. Without correcting for reddening, the absolute magnitude at peak is approximately -18.24 mag in the *o*-band, and the light curve roughly resembles that of a Type Ia supernova, albeit with significant scatter. Considering possible reddening, the peak absolute magnitude and overall light curve shape are consistent with a Type Ia supernova (see Figure A1); however, the data are too noisy to draw a definitive conclusion for AT2023xsx.

2.2. AT2023xqy

AT2023xqy was first reported by ATLAS on November 13, 2023. Cross-matching with HyperLEDA indicated a projected offset of 9.86 arcseconds from the host galaxy’s core. The host galaxy of AT2023xqy is identified as PGC 72135, also known as ESO 408-16. This edge-on disk galaxy has a core that appears blurred due to extinction, suggesting that the core position provided by HyperLEDA may be inaccurate. Re-measuring the angular distance between AT2023xqy and the host galaxy core using DES DR10 *i*-band images yields approximately 8.60 arcseconds [Figure 1(c)]. PGC 72135 has a spectroscopic redshift measurement from 2dF of 0.0390, corresponding to a luminosity distance of 178.6 Mpc, which is in good agreement with the 165 Mpc distance estimated by [Niu et al. \(2025\)](#). We find that the projected distance of AT2023xqy from the host galactic center of approximately 6.9 kpc, making a tidal disruption event unlikely, as such events typically occur in the immediate vicinity of the galactic nucleus ([van Velzen et al. 2020](#)). The above coincidences indicate that AT2023xqy may be a plausible candidate for the EM counterpart of BNS merger candidate GW231109_235456.

The discovery magnitude of AT2023xqy reported on TNS was 19.32 mag in the GOTO *L* band. We also extracted its light curve from the high-cadence ATLAS data. Similar to AT2023xsx, AT2023xqy lacks observations in the *c*-band, so we adopted ATLAS *o*-band measurements. The light curve shows that AT2023xqy began brightening after its first 3σ detection at MJD 60259.097 and was securely detected above 5σ at MJD 60262.088, followed by a prolonged ~ 15 -day rise to peak brightness. The peak is relatively sharp, with the ATLAS *o*-band magnitude reaching 18.31 ± 0.11 mag. After the peak, the luminosity declined rapidly over ~ 5 days, followed by a plateau phase lasting at least 50 days. Due to a seasonal gap, no ATLAS observations were obtained

between MJD 60327.828 and 60424.145; by the end of this interval, AT2023xqy had faded below the ATLAS detection limit.

3. POSSIBLE ORIGIN OF AT2023xqy

Given the high-quality observation on the shape of the AT2023xqy light curve, we examine two possible scenarios to explain the origin of this transient phenomenon, a BNS merger-irrelevant scenario involving a peculiar supernova or a BNS merger-relevant scenario involving a magnetar-powered kilonova.

3.1. A BNS merger-irrelevant scenario?

The long-lasting (~ 100 days) light curve evolution may naturally suggest us a BNS merger-irrelevant supernova origin of AT2023xqy. However, as shown in Figure 2, we find that its peculiar feature may not be well-matched with typical supernova types. On the one hand, the peak absolute magnitude of AT2023xqy is -17.95 mag in the o -band, significantly fainter than that of Type Ia supernovae, even without reddening correction. On the other hand, AT2023xqy exhibits a plateau of 50-days, which may not be seen in Type Ib/Ic/II-L supernovae which display a rapidly declining single-peaked light curve feature after maximum luminosity (Taddia et al. 2015). Though this plateau may be observed in some superluminous supernovae (SLSNe), explained by a model with a central magnetar engine (e.g., Nicholl et al. 2017), their peak luminosity is an order of magnitude higher than that of AT2023xqy (Gal-Yam 2019), making it an unfavorable explanation.

The closest conventional analog Type II-P supernovae displaying comparable plateau features, also fails to fully account for the observed behavior. In Figure 2, we compare its light curve to Type II-P supernova templates recently constructed from 330 Type II-P supernovae observed by the Zwicky Transient Facility Census of the Local Universe survey (Das et al. 2025). Still, we observe a difference that AT2023xqy declines by ~ 0.6 mag from peak within ~ 5 days, whereas Type II-P supernovae typically exhibit only very weak declines (~ 0.1 mag) over the same period, which suggests that AT2023xqy does not resemble a typical Type II-P supernova.

Furthermore, we estimate the expected number of supernovae within the comoving volume of GW231109_235456 probed by LVK observations between the GW trigger time (MJD 60257.996) and the onset of AT2023xqy (MJD 60259.097–60262.088). Adopting the local volumetric supernova rates reported in Ma et al. (2025), which account for both Type I and II supernovae, we find an expectation value of ~ 0.01 – 0.05 events within two to four days after the BNS merger in

this volume. Under the assumption of Poissonian statistics, this corresponds to a relatively small probability of 1.0%–4.7% for a temporally coincident supernova occurring within the designated spatiotemporal window.

3.2. A BNS merger-relevant scenario?

As outlined in Section 2.2, the spatial alignment of AT2023xqy including its luminosity distance and rise time closely matches the localization constraints provided by the LVK GraceDB alert for GW231109_235456. Furthermore, compact binary population synthesis models integrated into cosmological hydrodynamic simulations (e.g., Chu et al. 2022) predicted a preferential association of BNS mergers with spiral galaxies of stellar mass around $10^{10} M_{\odot}$ at redshifts $z < 0.1$. Intriguingly, the host galaxy of AT2023xqy, ESO 408-16 (PGC 72135), is classified as an Sc-type galaxy with an absolute magnitude of -21.05 mag (Lauberts & Valentijn 1989), corresponding to a typical stellar mass of $\sim 1.4 \times 10^{10} M_{\odot}$, which is consistent with the above prediction. Additionally, BNS mergers typically exhibit spatial offsets from their host galaxy centers due to natal kicks imparted during the second supernova. AT2023xqy is offset by ~ 6.9 kpc from the center of ESO 408-16, a value well-aligned with the empirical distribution (Liu et al. 2023) derived from 27 short gamma-ray burst (sGRB) offsets reported in Fong et al. (2010) and Fong & Berger (2013). Taking together, these observational coincidences suggest that AT2023xqy may be a plausible EM counterpart candidate for the BNS merger GW231109_235456.

In principle, the main EM counterparts of BNS mergers in the Optical band are: (1) kilonovae, powered by the radioactive decay of the heavy elements, such as lanthanide elements synthesized via the r -process in the neutron-rich material ejecta (e.g., Li & Paczyński 1998; Metzger et al. 2010; Kasen et al. 2017); (2) afterglows, powered by the shock between the relativistic jet launched by the central engine and their ambient interstellar medium (e.g., Makhathini et al. 2021). However, the o -band peak magnitude of AT2023xqy ~ 18 mag is significantly brighter than the typical luminosity for both kilonova and afterglow signals placed at the same distance. For example, if we place the kilonova and afterglow associated with GW170817 at $d_L \sim 165$ Mpc, their peak magnitude is about $\sim 20/29$ mag. Moreover, the peak time of AT2023xqy is about ~ 15 days after the GW alert, which is significantly longer than the typical kilonova peak time of $\sim 1 - 2$ days but also significantly shorter than the typical afterglow peak time of $\sim 100 - 200$ days. Owing to the above two reasons, we conclude that the light curve of AT2023xqy is diffi-

cult to reconcile with standard kilonova and afterglow signals.

Here we propose a possible magnetar-powered kilonova scenario to explain the light curve of AT2023xqy. In principle, the remnant of the BNS merger may be a rapidly rotating magnetar or a black hole (e.g., Baiotti et al. 2008; Piro et al. 2017; Margalit et al. 2022; Salafia et al. 2022; Chen et al. 2025), depending on the component masses and equation of state (EOS) of BNS systems, which has been supported by both general relativistic hydrodynamic (GRMHD) simulations (e.g., Siegel & Metzger 2017; Musolino et al. 2025) and observations on sGRBs, including the extended emission (e.g., Metzger et al. 2008), X-ray flares (e.g., Campana et al. 2006) and the internal plateaus (e.g., Sun et al. 2023). In this magnetar scenario, the spin-down of the remnant magnetar supplies an additional energy through the strong magnetic wind (e.g., Dai et al. 2006; Fan & Xu 2006; Giacomazzo & Perna 2013; Yu et al. 2013), and thus may enhance the luminosity of the kilonova and extend its lasting time. By the toy model that the magnetar is surrounded by a quasi-spherical ejecta shell (more details can be seen in Appendix A), we find that the light curve of AT2023xqy may be explained by a central magnetar with typical spin period of $P_i \sim 27$ ms and magnetic field of $B \sim 1 \times 10^{15}$ G (e.g., Gao et al. 2016) with a flat temperature of ~ 3860 K, which can be seen in the red solid line in Figure 2. The settings of other parameters including the mass m_{ej} and velocity v_{ej} of the ejecta can be seen in Table A1. The first 15-day rise of the light curve comes from the blackbody radiation of the expanding ejecta, heated by both the radioactive decay and the magnetic wind from the magnetar and the subsequent rapid decay of 5-days is attributed by the ejecta cools down as it expands till reaching the floor temperature. The plateau emission lasting for at least 50 days is mainly powered by the stable spin-down energy injection.

Nevertheless, we should point out that there is a non-negligible caveat for the magnetar-powered kilonova scenario on the lifetime of the magnetar. Currently, the observations on sGRBs only provide the evidence on the existence of magnetar merger remnant with τ_{life} of several hundreds of seconds (e.g., Lü et al. 2015). However, the lifetime τ_{life} needed to recover the light curve of AT2023xqy should be within the range of $\sim [70, 160]$ days, otherwise the late plateau should suffer a sharp decay quickly or remains bright for ATLAS detection. One possible explanation is that the magnetar is a long-lived marginally-stable supramassive NS with mass $1.0M_{\text{TOV}} < M_{\text{NS}} \lesssim 1.2M_{\text{TOV}}$ (e.g., Breu & Rezzolla 2016). By the procedure given in Salafia et al. (2022),

we find that with the total mass of GW231109_235456 reported in Niu et al. (2025) $M_{\text{tot}} \sim 2.9M_{\odot}$, the mass of the merger remnant M_{NS} is around $\sim 2.6 - 2.8M_{\odot}$ depending on the mass ratio q , indicating a EOS of NS with large M_{TOV} such as AB-N and AB-L (e.g., Arnett & Bowers 1977), which is however much stiffer than that constrained by current available multi-messenger observations (e.g., Dietrich et al. 2020).

While the observed light curve can be reproduced by our model, we propose AT2023xqy as a plausible candidate for a magnetar-powered kilonova under extreme conditions, noting that this interpretation requires further observational confirmation. Specifically a further follow-up observation in the radio band will be significantly helpful in determining the nature of AT2023xqy, since the radio afterglow signals may also be enhanced by the existence of the magnetar central engine i.e., several ten times brighter than the standard afterglow (Gao et al. 2015), thus providing a critical diagnostics to either support or challenge this interpretation.

4. SUMMARY

In this letter, we carried out a systematic archival search for the EM counterparts of the BNS merger candidate GW231109_235456. By examining all transients reported within four days of the event and inside the 90% sky localization, we identified eight candidates. Among them, two (AT2023xsx and AT2023xqy) have host galaxies consistent with the inferred merger distance.

AT2023xqy, located at 178.6 Mpc, shows the best spatial and distance agreement with GW231109_235456. Furthermore, near the trigger time of GW231109_235456 (MJD 60257.996), AT2023xqy showed evidence of a ~ 15 -day rise, first detected at 3σ significance on MJD 60259.097 and confirmed above 5σ on MJD 60262.088. This was followed by a rapid ~ 5 -day decline and a plateau lasting at least 50 days, with the subsequent decay unobserved due to a data gap. The spatiotemporal coincidences indicate that AT2023xqy could be a candidate for the EM counterpart of BNS merger candidate GW231109_235456, though its lightcurve is difficult to reconcile with a standard kilonova.

We examine two possible scenarios for the origin of AT2023xqy, a BNS merger-irrelevant scenario involving a supernova or a BNS merger-relevant scenario involving a magnetar-powered kilonova. In the former scenario, AT2023xqy may not be clearly categorized to a certain type of known supernovae, though with close analog of Type II-P. In the latter scenario, a simple toy model suggests that the emission could arise from ejecta heated

by both radioactive decay and the spin-down energy of a nascent magnetar with an initial spin period of ~ 27 ms and a magnetic field of $\sim 10^{15}$ G.

With strong coincidence in both occurrence time and spatial distribution, though a peculiar supernova origin cannot be ruled out, AT2023xqy remains a plausible EM counterpart candidate to GW231109_235456, potentially representing the second GW EM counterpart candidate following AT2017gfo. This case, if confirmed, may indicate that the EM counterparts of BNS merger GW events exhibit broad diversity compared with GW170817, which may be considered in future searches. Follow-up radio observations are strongly encouraged, as they may provide critical diagnostics for the magnetar-powered interpretation.

ACKNOWLEDGMENTS

YH acknowledges the support from the National Science Foundation of China (NSFC grant No. 12422303), the Fundamental Research Funds for the Central Universities (grant Nos. 118900M122, E5EQ3301X2, and E4EQ3301X2), and the National Key R&D Programme of China (grant No. 2023YFA1608303). ZC acknowledges the Postdoctoral Fellowship Program of CPSF under Grant Number GZB20250735. YL acknowledges the support from the Strategic Priority Program of the Chinese Academy of Sciences (grant no. XDB 23040100), the National Natural Science Foundation of China (grant nos. 12273050 and 12533009), and the National Astronomical Observatory of China (grant no. E4TG660101). JFL acknowledges the support from the NSFC through grant Nos. of 11988101 and 11933004, and the New Cornerstone Science Foundation through the New Cornerstone Investigator Program and the XPLOER PRIZE.

This research has made use of the CfA Supernova Archive, which is funded in part by the National Science Foundation through grant AST 0907903.

APPENDIX

A. TOY MODEL OF MAGNETAR-POWERED KILONOVA

Suppose the magnetar is surrounded by a quasi-spherical ejecta shell with mass M_{ej} , the total kinetic energy of the system can be expressed as (e.g., Yu et al. 2013; Gao et al. 2015)

$$E = (\Gamma - 1)M_{\text{ej}} + \Gamma E'_{\text{int}} + (\Gamma^2 - 1)M_{\text{sw}}, \quad (\text{A1})$$

where Γ is the bulk Lorentz factor of the ejecta, M_{sw} is the swept mass from the interstellar medium, R is the radius of the ejecta, and E_{int} is the internal energy. Here and hereafter the symbols with prime represent the quantities measured in the comoving rest frame. Then the dynamical evolution of the ejecta can be determined with the following ordinary differential equations (ODEs)

$$\frac{d\Gamma}{dt} = \frac{\frac{dE}{dt} - \Gamma \mathcal{D} \left(\frac{dE'_{\text{int}}}{dt'} \right) - (\Gamma^2 - 1)c^2 \left(\frac{dM_{\text{sw}}}{dt} \right)}{M_{\text{ej}}c^2 + E'_{\text{int}} + 2\Gamma M_{\text{sw}}c^2}, \quad (\text{A2})$$

$$\frac{dE}{dt} = L_{\text{sd}} + \mathcal{D}^2 L'_{\text{ra}} - \mathcal{D}^2 L'_e. \quad (\text{A3})$$

$$\frac{dE'_{\text{int}}}{dt'} = \mathcal{D}^{-2} L_{\text{sd}} + L'_{\text{ra}} - L'_e - \frac{E'_{\text{int}}}{3V'} \frac{dV'}{dt'}, \quad (\text{A4})$$

$$\frac{dV'}{dt'} = 4\pi R^2 \beta c, \quad (\text{A5})$$

$$\frac{dR}{dt} = \frac{\beta c}{(1 - \beta)}. \quad (\text{A6})$$

Table A1. Model parameters adopted for recovering the light curves of AT2023xqy

Parameter	Name	Value
m_{ej}	Ejecta mass	$4 \times 10^{-3} M_{\odot}$
v_{ej}	Ejecta velocity	$0.1 c$
κ	Opacity	10 g/cm^2
P_i	Magnetar period	27 ms
B	Magnetic field	10^{15} G
R_s	Magnetar radii	11 km
T_f	Floor Temperature	3860 K

In the above equations, $\mathcal{D} = 1/[\Gamma(1 - \beta)]$ is the Doppler factor with $\beta = \sqrt{1 - \Gamma^{-2}}$, and the comoving time dt' can be estimated from the observer frame time dt by $dt' = \mathcal{D}dt$. The term L_{ra} is the r-process power given by

$$L'_{\text{ra}} = 4 \times 10^{49} M_{\text{ej},-2} \left[\frac{1}{2} - \frac{1}{\pi} \arctan \left(\frac{t' - t'_0}{t'_\sigma} \right) \right]^{1.3} \text{ erg s}^{-1}, \quad (\text{A7})$$

with $t'_0 \sim 1.3 \text{ s}$ and $t'_\sigma \sim 0.11 \text{ s}$ (e.g., Korobkin et al. 2012) and hereafter the convention $Q_x = Q/10^x$ is adopted in cgs units. The term L'_e is the luminosity emitted, which can be written as

$$L'_e = \begin{cases} \frac{E'_{\text{int}} c}{\tau R/\Gamma}, \tau > 1, \\ \frac{E'_{\text{int}} c}{R/\Gamma}, \tau < 1, \end{cases} \quad (\text{A8})$$

where $\tau = \kappa(M_{\text{ej}}/V')(R/\Gamma)$ is the optical depth of the ejecta with opacity κ (e.g., Kasen & Bildsten 2010). The term L_{sd} is the spin-down energy of the central magnetar remnant assuming an isotropic Poynting flux, which can be written as

$$L_{\text{sd}} = L_{\text{sd},i} \left(1 + \frac{t}{t_{\text{sd}}} \right)^{-2}, \quad (\text{A9})$$

where $L_{\text{sd},i} = 10^{47} R_{s,6}^6 B_{14}^2 P_{i,-3}^{-4} \text{ erg s}^{-1}$ is the initial spin-down luminosity, and $t_{\text{sd}} = 2 \times 10^5 R_{s,6}^{-6} B_{14}^{-2} P_{i,-3}^2 \text{ s}$ is the spin-down timescale (e.g., Dai et al. 2006; Fan & Xu 2006; Giacomazzo & Perna 2013; Yu et al. 2013), with R_s , B and P_i representing the radius, magnetic field, and initial spin period of the magnetar. Then, the temperature of the expanding ejecta can be estimated directly by $T' = (E'_{\text{int}}/aV')^{1/4}$, where a is the radiation constant. Assuming a blackbody spectrum for the thermal emission of the mergernova, for a certain observational frequency ν , the observed flux can be calculated as

$$F_\nu = \frac{1}{4\pi D_L^2 \max(\tau, 1)} \frac{8\pi^2 \mathcal{D}^2 R^2}{h^3 c^2 \nu} \frac{(h\nu/\mathcal{D})^4}{\exp(h\nu/\mathcal{D}kT') - 1}, \quad (\text{A10})$$

where h is the Planck constant and D_L is the luminosity distance. Following the supernova modeling with magnetar central engine (e.g., Nicholl et al. 2017), we introduce a flat temperature T_f , i.e., once the temperature T' decreases to T_f with the expansion of the ejecta, the temperature will remain constant (i.e., isothermal expansion) and the ejecta radius evolves with $R = (3E_{\text{int}}/4\pi a T_f^4)^{1/3}$ after this value.

B. LIGHT CURVE OF AT2023XSZ

Figure A1 shows the light curve of AT2023xsx, compared with template light curves of various transient types.

REFERENCES

- Aasi, J., et al. 2015, *Class. Quant. Grav.*, 32, 074001, doi: [10.1088/0264-9381/32/7/074001](https://doi.org/10.1088/0264-9381/32/7/074001)
- Abbott, B. P., et al. 2017a, *Phys. Rev. Lett.*, 119, 161101, doi: [10.1103/PhysRevLett.119.161101](https://doi.org/10.1103/PhysRevLett.119.161101)
- Abac, A. G., et al. 2025. <https://arxiv.org/abs/2508.18082>

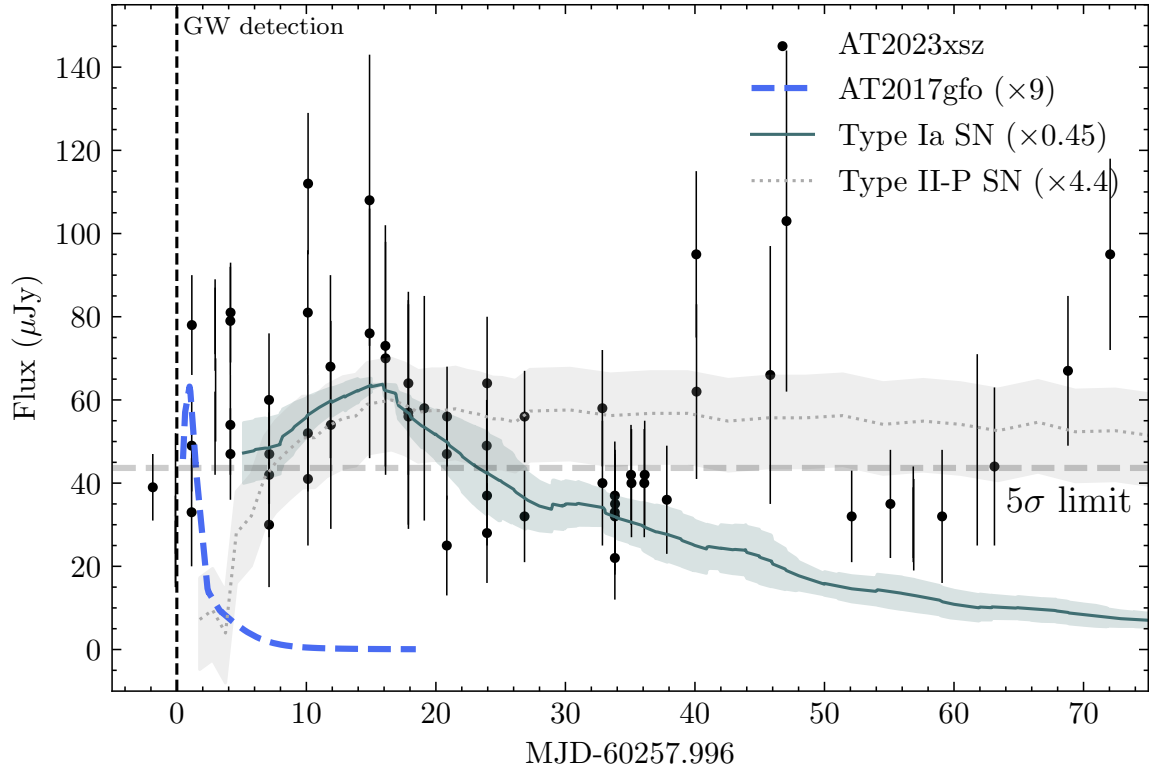


Figure A1. Similar to Figure 2 but for AT2023xsx. However, we did not apply our toy model to AT2023xsx due to its relatively low photometric quality. Only photometric measurements above the 2σ detection threshold are shown here.

- . 2017b, *Astrophys. J. Lett.*, 848, L12,
doi: [10.3847/2041-8213/aa91c9](https://doi.org/10.3847/2041-8213/aa91c9)
- Abbott, B. P., Abbott, R., Abbott, T. D., et al. 2017c, *ApJL*, 848, L12, doi: [10.3847/2041-8213/aa91c9](https://doi.org/10.3847/2041-8213/aa91c9)
- Abbott, B. P., et al. 2020, *Astrophys. J. Lett.*, 892, L3, doi: [10.3847/2041-8213/ab75f5](https://doi.org/10.3847/2041-8213/ab75f5)
- Acernese, F., et al. 2015, *Class. Quant. Grav.*, 32, 024001, doi: [10.1088/0264-9381/32/2/024001](https://doi.org/10.1088/0264-9381/32/2/024001)
- Arnett, W. D., & Bowers, R. L. 1977, *ApJS*, 33, 415, doi: [10.1086/190434](https://doi.org/10.1086/190434)
- Baiotti, L., Giacomazzo, B., & Rezzolla, L. 2008, *PhRvD*, 78, 084033, doi: [10.1103/PhysRevD.78.084033](https://doi.org/10.1103/PhysRevD.78.084033)
- Breu, C., & Rezzolla, L. 2016, *MNRAS*, 459, 646, doi: [10.1093/mnras/stw575](https://doi.org/10.1093/mnras/stw575)
- Campana, S., Mangano, V., Blustin, A. J., et al. 2006, *Nature*, 442, 1008, doi: [10.1038/nature04892](https://doi.org/10.1038/nature04892)
- Capote, E., et al. 2025, *Phys. Rev. D*, 111, 062002, doi: [10.1103/PhysRevD.111.062002](https://doi.org/10.1103/PhysRevD.111.062002)
- Chen, Z., Lu, Y., Ma, H., & Chu, Q. 2025, submitted to *MNRAS*
- Chu, Q., Yu, S., & Lu, Y. 2022, *MNRAS*, 509, 1557, doi: [10.1093/mnras/stab2882](https://doi.org/10.1093/mnras/stab2882)
- Colless, M., Dalton, G., Maddox, S., et al. 2001, *MNRAS*, 328, 1039, doi: [10.1046/j.1365-8711.2001.04902.x](https://doi.org/10.1046/j.1365-8711.2001.04902.x)
- Cowperthwaite, P. S., Berger, E., Villar, V. A., et al. 2017, *The Astrophysical Journal*, 848, L17, doi: [10.3847/2041-8213/aa8fc7](https://doi.org/10.3847/2041-8213/aa8fc7)
- Dai, Z. G., Wang, X. Y., Wu, X. F., & Zhang, B. 2006, *Science*, 311, 1127, doi: [10.1126/science.1123606](https://doi.org/10.1126/science.1123606)
- Dark Energy Survey Collaboration, Abbott, T., Abdalla, F. B., et al. 2016, *MNRAS*, 460, 1270, doi: [10.1093/mnras/stw641](https://doi.org/10.1093/mnras/stw641)
- Das, K. K., Kasliwal, M. M., Fremling, C., et al. 2025, *Low-Luminosity Type IIP Supernovae from the Zwicky Transient Facility Census of the Local Universe. I: Luminosity Function, Volumetric Rate.* <https://arxiv.org/abs/2502.19493>
- Das, K. K., Kasliwal, M. M., Fremling, C., et al. 2025, *PASP*, 137, 044203, doi: [10.1088/1538-3873/adcaeb](https://doi.org/10.1088/1538-3873/adcaeb)
- Dietrich, T., Coughlin, M. W., Pang, P. T. H., et al. 2020, *Science*, 370, 1450, doi: [10.1126/science.abb4317](https://doi.org/10.1126/science.abb4317)
- Dyer, M. J., Ackley, K., Jiménez-Ibarra, F., et al. 2024, *The Gravitational-wave Optical Transient Observer (GOTO).* <https://arxiv.org/abs/2407.17176>
- Fan, Y.-Z., & Xu, D. 2006, *MNRAS*, 372, L19, doi: [10.1111/j.1745-3933.2006.00217.x](https://doi.org/10.1111/j.1745-3933.2006.00217.x)
- Fong, W., & Berger, E. 2013, *ApJ*, 776, 18, doi: [10.1088/0004-637X/776/1/18](https://doi.org/10.1088/0004-637X/776/1/18)

- Fong, W., Berger, E., & Fox, D. B. 2010, *ApJ*, 708, 9, doi: [10.1088/0004-637X/708/1/9](https://doi.org/10.1088/0004-637X/708/1/9)
- Gal-Yam, A. 2019, *Annual Review of Astronomy and Astrophysics*, 57, 305–333, doi: [10.1146/annurev-astro-081817-051819](https://doi.org/10.1146/annurev-astro-081817-051819)
- Ganapathy, D., et al. 2023, *Phys. Rev. X*, 13, 041021, doi: [10.1103/PhysRevX.13.041021](https://doi.org/10.1103/PhysRevX.13.041021)
- Gao, H., Ding, X., Wu, X.-F., Dai, Z.-G., & Zhang, B. 2015, *ApJ*, 807, 163, doi: [10.1088/0004-637X/807/2/163](https://doi.org/10.1088/0004-637X/807/2/163)
- Gao, H., Zhang, B., & Lü, H.-J. 2016, *Phys. Rev. D*, 93, 044065, doi: [10.1103/PhysRevD.93.044065](https://doi.org/10.1103/PhysRevD.93.044065)
- Giacomazzo, B., & Perna, R. 2013, *ApJL*, 771, L26, doi: [10.1088/2041-8205/771/2/L26](https://doi.org/10.1088/2041-8205/771/2/L26)
- Gill, R., Nathanael, A., & Rezzolla, L. 2019, *ApJ*, 876, 139, doi: [10.3847/1538-4357/ab16da](https://doi.org/10.3847/1538-4357/ab16da)
- Jha, S., Kirshner, R. P., Challis, P., et al. 2006, *AJ*, 131, 527, doi: [10.1086/497989](https://doi.org/10.1086/497989)
- Kaiser, N., Aussel, H., Burke, B. E., et al. 2002, in *Society of Photo-Optical Instrumentation Engineers (SPIE) Conference Series*, Vol. 4836, *Survey and Other Telescope Technologies and Discoveries*, ed. J. A. Tyson & S. Wolff, 154–164, doi: [10.1117/12.457365](https://doi.org/10.1117/12.457365)
- Kasen, D., & Bildsten, L. 2010, *ApJ*, 717, 245, doi: [10.1088/0004-637X/717/1/245](https://doi.org/10.1088/0004-637X/717/1/245)
- Kasen, D., Metzger, B., Barnes, J., Quataert, E., & Ramirez-Ruiz, E. 2017, *Nature*, 551, 80, doi: [10.1038/nature24453](https://doi.org/10.1038/nature24453)
- Korobkin, O., Rosswog, S., Arcones, A., & Winteler, C. 2012, *MNRAS*, 426, 1940, doi: [10.1111/j.1365-2966.2012.21859.x](https://doi.org/10.1111/j.1365-2966.2012.21859.x)
- Lauberts, A., & Valentijn, E. A. 1989, *The surface photometry catalogue of the ESO-Uppsala galaxies*
- Li, L.-X., & Paczyński, B. 1998, *ApJL*, 507, L59, doi: [10.1086/311680](https://doi.org/10.1086/311680)
- Liu, Z.-Y., Lin, Z.-Y., Yu, J.-M., et al. 2023, *ApJ*, 947, 59, doi: [10.3847/1538-4357/acc73b](https://doi.org/10.3847/1538-4357/acc73b)
- Lü, H.-J., Zhang, B., Lei, W.-H., Li, Y., & Lasky, P. D. 2015, *ApJ*, 805, 89, doi: [10.1088/0004-637X/805/2/89](https://doi.org/10.1088/0004-637X/805/2/89)
- Ma, X., Wang, X., Mo, J., et al. 2025, *A&A*, 698, A306, doi: [10.1051/0004-6361/202452685](https://doi.org/10.1051/0004-6361/202452685)
- Makhathini, S., Mooley, K. P., Brightman, M., et al. 2021, *ApJ*, 922, 154, doi: [10.3847/1538-4357/ac1ffc](https://doi.org/10.3847/1538-4357/ac1ffc)
- Margalit, B., Jermyn, A. S., Metzger, B. D., Roberts, L. F., & Quataert, E. 2022, *ApJ*, 939, 51, doi: [10.3847/1538-4357/ac8b01](https://doi.org/10.3847/1538-4357/ac8b01)
- Metzger, B. D., Quataert, E., & Thompson, T. A. 2008, *MNRAS*, 385, 1455, doi: [10.1111/j.1365-2966.2008.12923.x](https://doi.org/10.1111/j.1365-2966.2008.12923.x)
- Metzger, B. D., Martínez-Pinedo, G., Darbha, S., et al. 2010, *MNRAS*, 406, 2650, doi: [10.1111/j.1365-2966.2010.16864.x](https://doi.org/10.1111/j.1365-2966.2010.16864.x)
- Mooley, K. P., Deller, A. T., Gottlieb, O., et al. 2018, *Nature*, 561, 355, doi: [10.1038/s41586-018-0486-3](https://doi.org/10.1038/s41586-018-0486-3)
- Musolino, C., Rezzolla, L., & Most, E. R. 2025, *ApJL*, 984, L61, doi: [10.3847/2041-8213/adcd6d](https://doi.org/10.3847/2041-8213/adcd6d)
- Nicholl, M., Guillochon, J., & Berger, E. 2017, *ApJ*, 850, 55, doi: [10.3847/1538-4357/aa9334](https://doi.org/10.3847/1538-4357/aa9334)
- Niu, W., Hanna, C., Haster, C.-J., et al. 2025, *arXiv e-prints*, arXiv:2509.09741, <https://arxiv.org/abs/2509.09741>
- Özel, F., & Freire, P. 2016, *ARA&A*, 54, 401, doi: [10.1146/annurev-astro-081915-023322](https://doi.org/10.1146/annurev-astro-081915-023322)
- Paturel, G., Petit, C., Prugniel, P., et al. 2003, *A&A*, 412, 45, doi: [10.1051/0004-6361:20031411](https://doi.org/10.1051/0004-6361:20031411)
- Piro, A. L., Giacomazzo, B., & Perna, R. 2017, *ApJL*, 844, L19, doi: [10.3847/2041-8213/aa7f2f](https://doi.org/10.3847/2041-8213/aa7f2f)
- Planck Collaboration, Aghanim, N., Akrami, Y., et al. 2020, *A&A*, 641, A6, doi: [10.1051/0004-6361/201833910](https://doi.org/10.1051/0004-6361/201833910)
- Salafia, O. S., Colombo, A., Gabrielli, F., & Mandel, I. 2022, *A&A*, 666, A174, doi: [10.1051/0004-6361/202243260](https://doi.org/10.1051/0004-6361/202243260)
- Sánchez, C., Carrasco Kind, M., Lin, H., et al. 2014, *MNRAS*, 445, 1482, doi: [10.1093/mnras/stu1836](https://doi.org/10.1093/mnras/stu1836)
- Siegel, D. M., & Metzger, B. D. 2017, *PhRvL*, 119, 231102, doi: [10.1103/PhysRevLett.119.231102](https://doi.org/10.1103/PhysRevLett.119.231102)
- Smith, K. W., Smartt, S. J., Young, D. R., et al. 2020, *PASP*, 132, 085002, doi: [10.1088/1538-3873/ab936e](https://doi.org/10.1088/1538-3873/ab936e)
- Soni, S., et al. 2025, *Class. Quant. Grav.*, 42, 085016, doi: [10.1088/1361-6382/adc4b6](https://doi.org/10.1088/1361-6382/adc4b6)
- Sun, H., Wang, C. W., Yang, J., et al. 2023, *arXiv e-prints*, arXiv:2307.05689, doi: [10.48550/arXiv.2307.05689](https://doi.org/10.48550/arXiv.2307.05689)
- Taddia, F., Sollerman, J., Leloudas, G., et al. 2015, *Astronomy & Astrophysics*, 574, A60, doi: [10.1051/0004-6361/201423915](https://doi.org/10.1051/0004-6361/201423915)
- Tonry, J. L., Denneau, L., Heinze, A. N., et al. 2018, *PASP*, 130, 064505, doi: [10.1088/1538-3873/aabadf](https://doi.org/10.1088/1538-3873/aabadf)
- van Velzen, S., Holoien, T. W. S., Onori, F., Hung, T., & Arcavi, I. 2020, *SSRv*, 216, 124, doi: [10.1007/s11214-020-00753-z](https://doi.org/10.1007/s11214-020-00753-z)
- Yu, Y.-W., Zhang, B., & Gao, H. 2013, *ApJL*, 776, L40, doi: [10.1088/2041-8205/776/2/L40](https://doi.org/10.1088/2041-8205/776/2/L40)